Prediction of hydrocyclone performance using artificial neural networks

by M. Karimi*, A. Dehghani*, A. Nezamalhosseini*, and Sh. Talebi*

Synopsis

Artificial neural networks (ANNs) have found their applications in the modelling of unit operations of mineral processing plants. In this research, laboratory-scale tests were conducted, using a three-inch diameter Mozley hydrocyclone. Main parameters included pressure drop at inlet, solid per cent, vortex and apex diameter were adjusted. The corrected cut size (d_{50c}) and the flow rates of underflow and overflow were determined. Multi layers perceptron (MLP) feed forward network architectures were designed to predict the responses. The results showed a good correlation between experimental and network output, for corrected cut size and flow rates.

Keywords: hydrocyclone, artificial neural network, corrected cut size, flow rates.

Introduction

The hydrocyclone is one of the most versatile types of industrial centrifugal separators. Due to its simple design, low cost, easy operation and low floor space requirement, the hydrocyclone has found an important role in mineral processing plants as a solid-liquid separator. A typical hydrocyclone consists of a conical shape vessel, open at its apex, or underflow, joined to a cylindrical section which has a tangential feed inlet (Wills, 1997).

Two of the fundamental parameters that are used for representing hydrocyclone efficiency include: cut size, d_{50}, which represents the size of particles that have an equal chance of going either with the overflow or underflow, and flow recovery to underflow, R_f, which depends on flow rates to overflow (O_f) and underflow (U_f) (Svarovsky, 1984). A partition curve is used to determine d_{50}, which provides the relationship between the weight fraction of each particle size in the overflow and underflow streams. Flow recovery to the underflow is calculated from the dilution rates of three streams. In practical applications, the d_{50} is corrected by assuming that a fraction of the heavier particles are entrained in the overflow system, which is equivalent to the fraction of water in the underflow. This correction of d_{50} is designated as d_{50c} (Figure 1).

Mathematically, the d_{50c} and R_f can be estimated by empirical models such as Lynch and Nageswararao (Lynch, 1997). However, empirical models are not able to consider all the effective parameters. Artificial neural networks (ANNs) were used to predict d_{50c} (Eren *et al*. 1996). Many nonconventional operational variables such as water and solid split ratios, overflow and underflow densities, and apex and vortex flow rates were considered as the input parameters. Wander Waltt (1993) has introduced a 'feed forward neural network' as a useful tool for modelling in minerals engineering and the prediction of a hydrocyclone partition curve.

In this research, the d_{50c} and flow rates of underflow and overflow have been predicted, using ANNs. Pressure drop at inlet, feed solid per cent, vortex and apex diameters have been selected as network input parameters. The overall performance of the hydrocyclone has been validated by the analysis of the correlation coefficient (R^2), mean square error (MSE), and comparison of predicted and actual values.

Experiments

Laboratory-scale tests were conducted, using a three-inch diameter Mozley hydrocyclone. An experimental design method was employed in conducting the tests. In each test, the main input parameters were adjusted and samples from feed, overflow, and underflow were collected (Figure 2). Feed with different solid per cent was prepared. Samples from each

* Department of Mining and Metalllurgical Engineering, Yazd University, Yazd, Iran.

 Paper received Jun. 2009; revised paper received Dec. 2009.

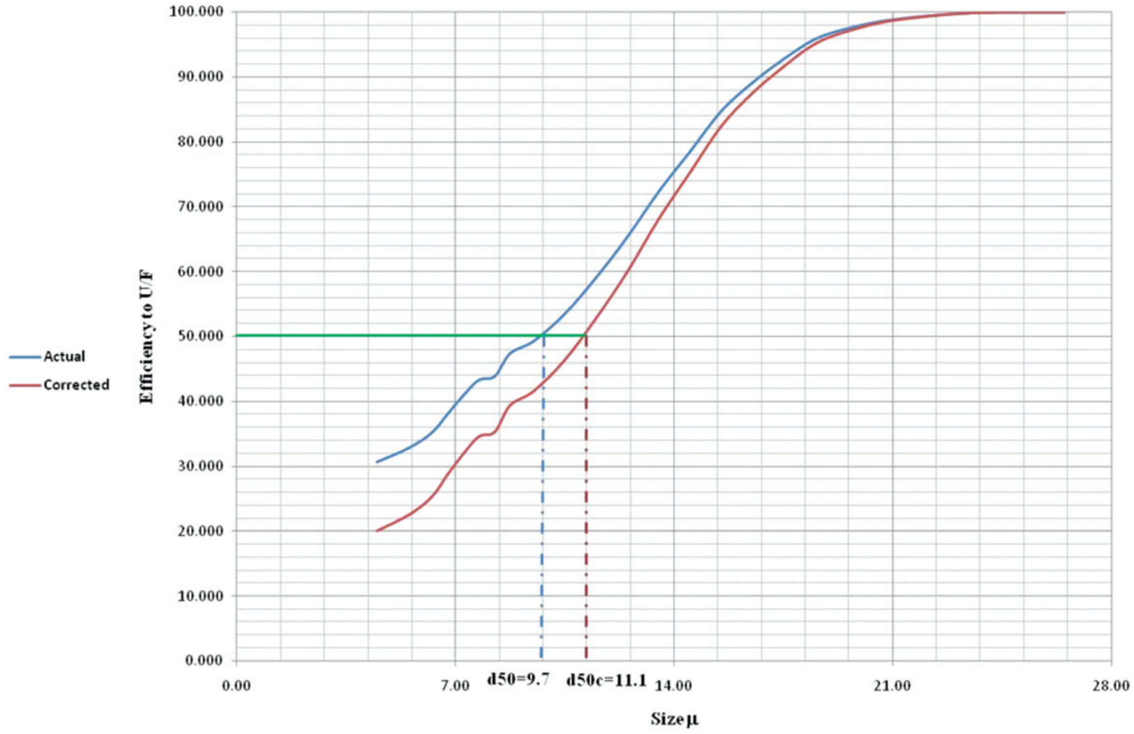

Figure 1—Corrected vs. actual cut size for test No. 7

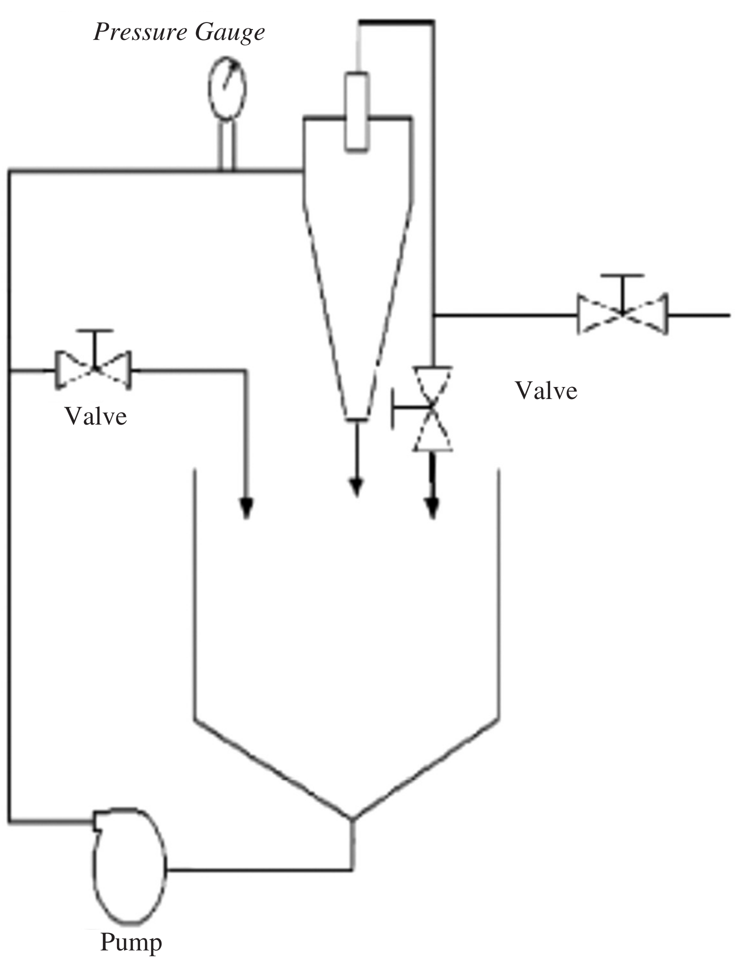

Figure 2—Schematic diagram of the experimental setup

steam were taken, when the hydrocyclone was working in a steady-state condition. A laser diffraction method was used to determine the size distribution of samples. The performance parameters were then calculated.

Result and discussion

The d_{50c}, U_f and O_f, were used as output variables. In order to estimate these variables, parameters such as pressure drop at inlet, solid per cent, vortex and apex diameter, were used as input variables. The complex relationship between input and output patterns was captured through a network via a set of connection weights, which were adjusted during training of the networks. The network captures an input-output relationship through training and acquires a certain prediction capability to produce an output for a given input.

In order to decrease error and increase generalization capability, two separate networks were designed, for the prediction of corrected cut size, and U_f and O_f. In the following paragraphs the procedures of designing optimal networks is explained.

Corrected cut size prediction

The network architecture used for analysis was a multilayer perceptron (MLP) feed forward neural network. The MLP architecture is capable of employing different activation functions in hidden and output layers. The MLP used for the prediction of d_{50c} has three layers: the input layer, one hidden layer, and the output layer. The selected optimized network includes 4 neurons in the hidden layer (Figure 3). Among various activation functions available, such as tanh, threshold, linear, sigmoid and Gaussian, the logistic sigmoid function showed the best performance for activation of the hidden layer.

To train a neural network for prediction purposes and evaluate its performance, at least three data-sets, training, cross validation and test, are necessary. Therefore, 30 sets of data were subdivided into three subsets, 19 training, 6 cross validation and 5 test data (see Appendix A). Table I presents the results of the optimized MLP on the test data used for prediction of the output.

In order to compare the results, four statistical indices including mean squared error (MSE), normalized mean squared error (NMSE), mean absolute error (MAE), and R^2 were used to compare the results. MSE is the mean of the squared deviation between the actual and the estimation. It is a measure of accuracy for estimation, which takes into account both the bias and the error variance. MAE measures the average absolute deviation between actual and the estimate. R^2 is an evaluator for the percentage of variation of the actual data explained by the predicted data. It was observed (Table II) that the selected MLP demonstrated a good prediction of d_{50c}.

The comparison of the experimental and the predicted values with MLP is graphically shown in Figure 4. This figure illustrates a good estimation of hydrocyclone d_{50c}, using the multilayer perceptron neural network.

Prediction of flow rates to underflow and overflow

In order to design optimum net, several trial and error tests were conducted. An MLP network with 4-2-2 architecture was selected for prediction purposes (Figure 5.). A logistic sigmoid function was used for activation of the hidden layer. Optimized neural networks, which are applied for hydrocyclone performance prediction, have only one hidden layer, with a small number of hidden units; therefore they are able to produce appropriate results in a very short time.

Table I

d_{50c} network evaluation using test data

Pressure drop (psi)	Solid %	Vortex diameter (mm)	Apex diameter (mm)	d_{50}	d_{50} output
17.5	6	19	16.25	5.79	4.78
15	4	25	20	7.65	6.50
17.5	6	19	23.75	11.64	8.93
17.5	6	19	16.25	5.09	4.78
17.5	6	19	16.25	6	4.78

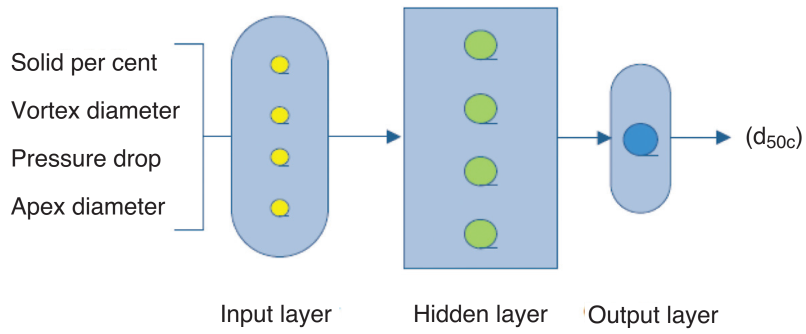

Figure 3—Optimized MLP architecture for d_{50c}

Table II

Statistical results for d_{50c}

Performance	Cut size
MSE	2.264
NMSE	0.407
MAE	1.284
Min abs error	0.313
Max abs error	2.715
R^2	0.977

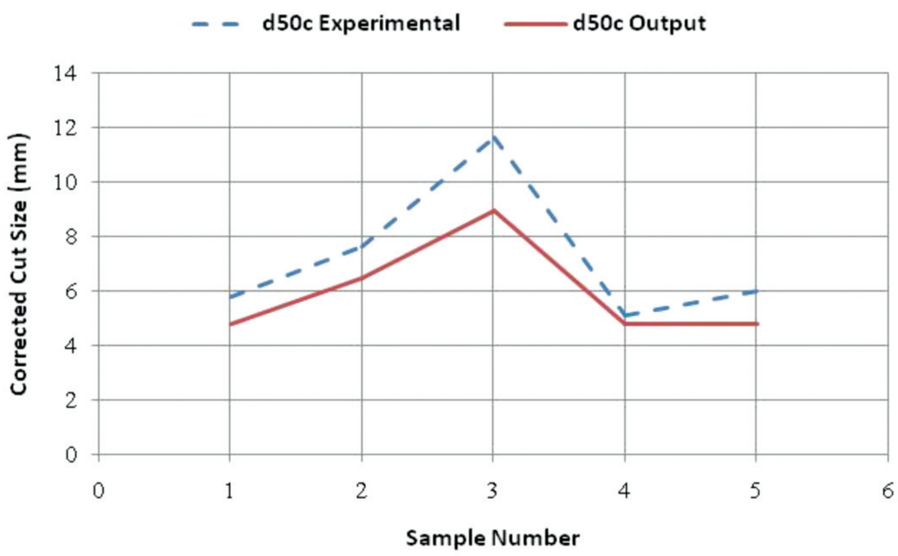

Figure 4—Measured and predicted d_{50c}, for test data set

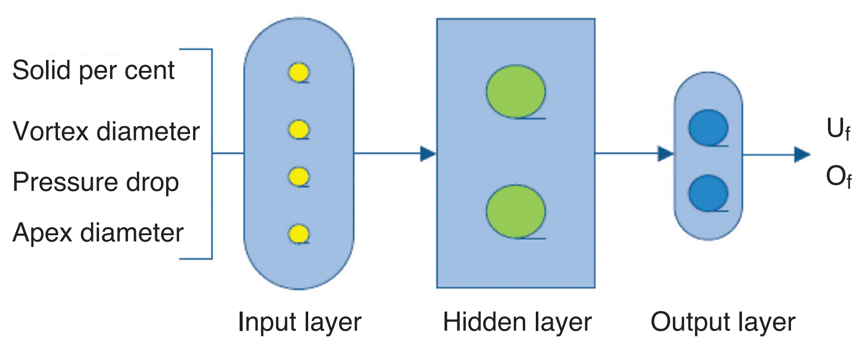

Figure 5—Optimized MLP architecture for U_f and O_f

The same data-set was applied for training, validation and test purposes (Appendix A). Table III demonstrates the results of the optimized MLP on the test data used for the prediction of U_f and O_f.

Statistical parameters were calculated (Table IV) and revealed that ANN is highly capable of estimating the flow rates.

Figures 6 and 7 display the measured versus output data for hydrocyclone underflow and overflow flow rates. According to these figures, the selected network has enough accuracy for underflow and overflow flow rates' approximation.

Conclusions

In this paper, the application of artificial neural networks, using two feed forward neural networks, for the estimation of the hydrocyclone corrected cut size (d_{50c}) and underflow (U_f)

Table III

U_f and O_f network evaluation using test data

Pressure drop (psi)	Solid per cent	Vortex diameter (mm)	Apex diameter (mm)	Underflow flow rate (t/h)	Overflow flow rate (t/h)	Underflow flow rate (t/h) Output	Overflow flow rate (t/h) Output
20	4	13	12.5	2.41	1.59	2.43	2.05
17.5	6	19	16.25	2.85	2.98	2.82	3.20
20	8	25	12.5	1.48	6.05	1.44	5.63
20	4	13	20	4.67	0.18	5.20	0.43
20	4	25	20	3.60	4.41	4.16	4.31

Table IV

Statistical results for U_f and O_f

Performance	Underflow flow rate	Overflow flow rate
MSE	0.119	0.124
NMSE	0.102	0.029
MAE	0.237	0.334
Min abs error	0.026	0.092
Max abs error	0.558	0.454
R^2	0.989	0.994

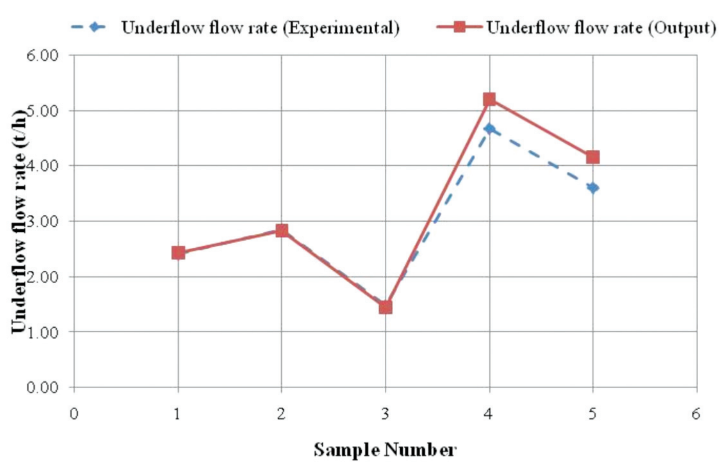

Figure 6—Measured and predicted U_f, for test data-set

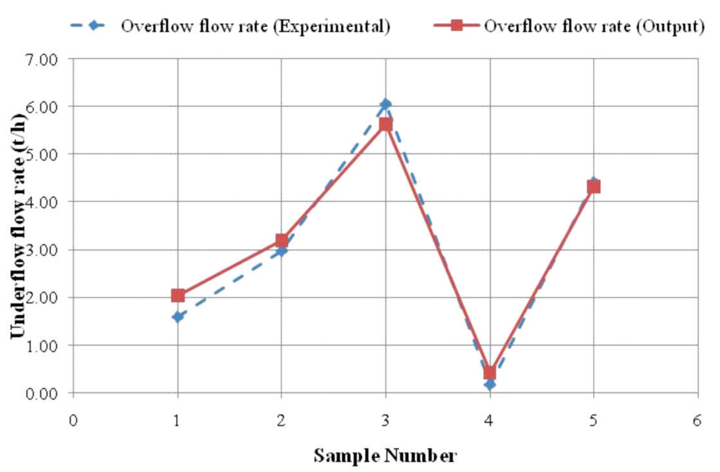

Figure 7—Measured and predicted O_f, for test data-set

and overflow (O_f) flow rates was investigated. The effects of input parameters such as pressure drop at inlet, solid per cent, vortex and apex diameter, were evaluated, using a laboratory-scale hydrocyclone. The d_{50c} was estimated, with an R-squared value of 97.7%, using an optimized three-layer perceptron, with 4-4-1 architecture. Also an optimized three - layers perceptron with 4-2-2 architecture could predict the U_f and O_f, with R-squared values of 98.9% and 99.4%, respectively. Promising results can be obtained using ANNs for efficient automatic control of hydrocyclones.

References

EREN, H., FUNG, CH., WONG, K., and GUPTA A. Artificial Neural Networks in estimation of hydrocyclone parameter d_{50c} with unusual input variables. *IEEE* 46, 1996, pp. 908–912.

LYNCH, A.J. *Mineral crushing and grinding circuits their simulation, optimization, design and control*, 1977, Elsevier Scientific Publishing.

SVAROVSKY, L. *Hydrocyclones*. 1984, Lancaster, PA, USA Technomic.

NAPIER-MUNN, T.J., MORRELL, S., MORRISON, R.D., and KOJOVIC, T. *Mineral Comminution Circuits: Their Operation and Optimization*. 1996, Australia, JKMRC.

WANDER WALT, T.J. and BERNARD, E. *Neural nets for the simulation of mineral processing operations*, 1993, South Africa, Elsevier Scientific Publishing.

WILLS, B.A. *Mineral Processing Technology, An Introduction to the practical aspects of ore treatment and mineral processing*, 6th edition, 1992, Pergamon Press, Oxford.

Appendix A

Experimental data

Data separation	No.	Pressure drop (psi)	Solid per cent	Vortex diameter (mm)	Apex diameter (mm)	Underflow flow rate (t/h)	Overflow flow rate (t/h)	Cut size	Rf
Training	1	17.5	6	19	8.75	0.86	4.27	15.81	0.11
	2	17.5	6	19	16.25	2.89	3.08	6.74	0.46
	3	15	4	13	20	4.16	0.11	13.98	0.85
	4	20	4	13	20	4.67	0.18	12.64	0.91
	5	15	4	25	20	3.20	3.80	7.65	0.47
	6	17.5	2	19	16.25	2.61	2.94	5.89	0.44
	7	20	4	13	12.5	2.41	1.59	1.94	0.52
	8	12.5	6	19	16.25	2.36	2.40	6.32	0.47
	9	17.5	6	19	16.25	2.85	2.98	6.00	0.51
	10	20	8	25	12.5	1.48	6.05	9.75	0.14
	11	22.5	6	19	16.25	3.23	3.44	9.74	0.48
	12	17.5	6	19	16.25	2.85	3.01	4.28	0.47
	13	17.5	10	19	16.25	3.00	3.13	5.19	0.46
	14	17.5	6	19	16.25	5.59	5.99	5.43	0.44
	15	17.5	6	31	16.25	1.90	5.33	9.62	0.23
	16	17.5	6	19	16.25	2.74	2.94	5.09	0.47
	17	17.5	6	19	23.75	6.81	0.81	11.64	0.91
	18	20	4	25	20	3.60	4.41	6.65	0.47
	19	20	8	13	20	5.01	0.06	16.01	0.88
Validation	20	15	8	13	20	4.52	0.12	12.52	0.87
	21	20	8	13	12.5	2.43	1.52	2.32	0.53
	22	20	4	25	12.5	1.01	5.97	10.18	0.13
	23	15	8	25	12.5	1.53	5.11	11.09	0.16
	24	17.5	6	7	16.25	3.10	1.00	3.24	0.67
	25	20	8	25	20	3.92	4.60	5.68	0.46
Test	26	15	8	25	20	3.54	3.99	6.48	0.48
	27	15	4	13	12.5	2.00	1.25	2.16	0.50
	28	17.5	6	19	16.25	2.82	3.09	5.79	0.49
	29	15	4	25	12.5	1.02	5.05	11.08	0.13
	30	15	8	13	12.5	2.23	1.39	3.69	0.47